The 2010 IEEE/RSJ International Conference on
Intelligent Robots and Systems
October 18-22, 2010, Taipei, Taiwan

Steering of Pedal Wave of a Snake-like Robot by Superposition of Curvatures

Hiroya Yamada and Shigeo Hirose

Abstract— **A snake-like robot has an advantage in moving into a narrow space. Particularly "pedal wave", which is one of its locomotion styles, is suitable for entering a thin path. However, pedal wave have been used only for going straight in most of the prior studies. In particular horizontal steering of pedal wave by a real robot has not been investigated sufficiently. Therefore in this paper we studied a kinematically appropriate steering method of pedal wave using a continuous snake-like robot model. We proposed steering by superposition of a steering curvatures and a pedal wave's curvature, and investigated the condition of suitable steering curvature using kinematic simulations. The proposed steering method was verified by experiments with a real snake-like robot.**

I. INTRODUCTION

Generally speaking, there are a lot of spaces in our living environment which are difficult for us to enter because of limited room or obstacles. A machine which is equipped with camera and some tools and able to go through thin paths will help us in working in such environments. For example, this type of machines is potentially helpful for search and rescue in a disaster area and investigation of a pipeline. A snake-like robot, which has a slender body and a large number of bending joints, is hopeful as an all-purpose machine working in narrow environments. Since the first snake-like robot was developed in 1972[1], various snake-like robots have been realized so far.

Several locomotion styles for a snake-like robot such as lateral undulation and sidewinding are known until today. They have the different pros and cons; for example, lateral undulation, which is the most typical style of a snake's locomotion, is fast and efficient but not useful in a thin straight path and on a slippery surface because it requires a space for winding its body and footholds to push. On the other hand, "pedal wave" is known as a locomotion style suitable for such environment (Fig. 1), though it is relatively slow and inefficient. (We note that this style has been called such as "travelling wave locomotion (or gait)" in other literatures[2]. However, we have called it as "pedal wave", which is originally used for the locomotion of gastropods such as snails, because the feature that the vertical waves travel to the same direction as the movement is similar. In addition, sometimes this style has been called "rectilinear", however, it may be not suitable because the waves travel to the opposite direction to the movement in a real snake's rectilinear[3].) Therefore pedal wave is complementary to lateral undulation. So far many robots have realized pedal wave experimentally[4][5].

However, pedal wave has been used only for going straight on in most of the prior studies. Literature[2] is the only study that described the detailed kinematics of steering of pedal wave as far as we know. But, the proposed algorithm required a mechanism with extremely large degree of freedom and a program to solve the inverse kinematics in order to fit the robot into the path in real time, thus it haven't been applied to a real robot. Literatures[4][6] describes the adaptations of pedal wave to uneven terrain and verified them experimentally, however, horizontal steering was not realized. The reader may think this situation is a little strange, because it seems sufficient to control the joint angle only around the tips of pedal wave in order to steer. Actually this idea is possible, but not attractive. For example, when a robot is steering on a level surface with this method, the projection to the surface looks like connected straight line segments (Fig. 2). This shape is clearly disadvantageous to steering along a narrow path. In addition, the turning radius tends to be large because this method doesn't utilize the joints not being around the tips. Moreover, there is a problem of how to control the joint angle when a tip comes to the gap between 2 adjacent joints in terms of the control of a real robot. Therefore in this paper we study the steering of pedal wave using distributed curvature.

This paper is organized as follows: In section I, the background of research was described. In section II, we review the kinematic model of a continuous snake-like robot, which is the basis of discussion in this paper. In section III, the steering method by superposition of curvatures is proposed and the condition of steering curvatures is investigated. In section IV, the experiments to verify the method using a real robot are described. Finally section V concludes this research.

II. KINEMATICS OF A CONTINUOUS SNAKE-LIKE ROBOT

Until today various structures of snake-like robots have been proposed; e.g. a series of universal joints, or a series of 1 DoF bending joints whose joint axes are rolled by 90 deg. to the previous joint. Though these structures have deferent kinematics, the general kinematic features are common. Thus an abstract model which is able to approximate various structures is very efficient for studies about general problems of snake-like robots such as locomotion styles[1][7]. Recently

This work was not supported by any organization

H. Yamada is with Global Edge Institute, Tokyo Institute of Technology, 2-12-1 Ookayama, Meguro-ku, Tokyo, Japan yamada@robotics.mes.titech.ac.jp

S. Hirose is with Department of Mechanical and Aerospace Engineering, Tokyo Institute of Technology, 2-12-1 Ookayama, Meguro-ku, Tokyo, Japan Hirose@mes.titech.ac.jp

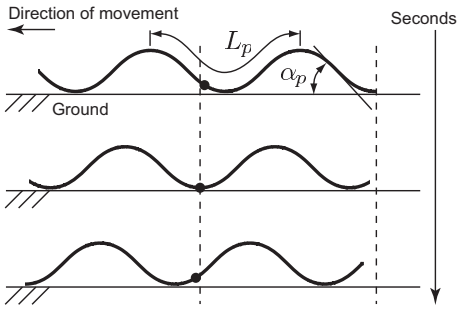

Fig. 1. Pedal wave of a snake-like robot (The point indicates the middle of the body)

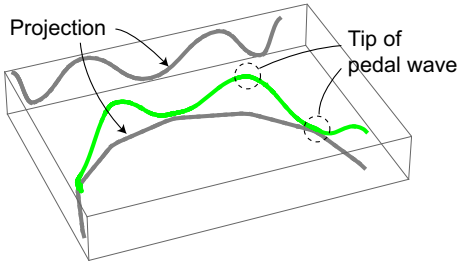

Fig. 2. Steering by controlling the joints only around the tips of pedal wave

we have proposed a continuous kinematic model inspired by the theory of a spatial curve, which we call a "dorsal reference curve", and clarified that it is able to approximate various structures of snake-like robots[8]. In this section we briefly review the mathematical definition of a dorsal reference curve.

A continuous curve is not enough to represent the shape of snake-like robot, because the robot has the distinction of the belly and the back[7]. Thus we have introduced differential equations extended from Frenet-Serret equations of a spatial curve, and called the solution as a "dorsal reference curve"[9][10]. A dorsal reference curve is a natural representation of an elongate body. Actually, the same idea was introduced for the study of elastica in the field of physics in 19th century[11].

The shape of a dorsal reference curve is explained by analogy of a track of an air plane (Fig. 3(a)). Now we consider a vector $\mathbf{c} = (x(s), y(s), z(s))$ as the position of the plane. s is a length of the track, therefore $s = 0$ means the starting point. An orthogonal frame $(\mathbf{e}_r(s), \mathbf{e}_p(s), \mathbf{e}_y(s))$ is considered as the posture of the plane, and $\mathbf{e}_r(s)$ (roll axis) is a unit vector facing the direction of movement, $\mathbf{e}_p(s)$ (pitch axis) is a unit vector facing to the direction of the left wing, and $\mathbf{e}_y(s)$ (yaw axis) is a unit vector facing to the direction of the vertical tail.

As a plane has an aileron, an elevator, and a rudder, we introduce 3 functions $\tau(s)$, $\kappa_p(s)$ and $\kappa_y(s)$ as the rotational velocity of rolling, pitching, and yawing respectively. These functions mean the difference of rotational angle [rad] when the plane travels for a unit length. Then, the track of the

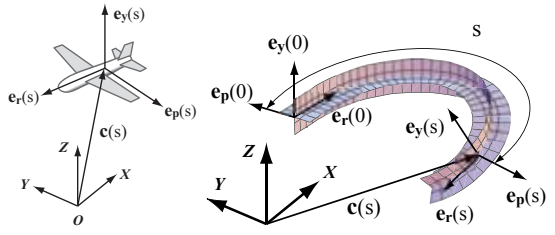

(a) Analogy with aircraft (b) A dorsal reference curve

Fig. 3. A dorsal reference curve

plane is calculated by following equations[9][10].

$$\begin{cases} \dfrac{d\mathbf{c}(s)}{ds} = \mathbf{e}_r(s) \\ \dfrac{d\mathbf{e}_r(s)}{ds} = \kappa_y(s)\mathbf{e}_p(s) - \kappa_p(s)\mathbf{e}_y(s) \\ \dfrac{d\mathbf{e}_p(s)}{ds} = -\kappa_y(s)\mathbf{e}_r(s) + \tau(s)\mathbf{e}_y(s) \\ \dfrac{d\mathbf{e}_y(s)}{ds} = \kappa_p(s)\mathbf{e}_r(s) - \tau(s)\mathbf{e}_p(s) \end{cases} \quad (1)$$

If the position $(\mathbf{c}(0))$ and the posture $(\mathbf{e}_r(0), \mathbf{e}_p(0), \mathbf{e}_y(0))$ at the starting point $(s = 0)$ and $\tau(s), \kappa_p(s), \kappa_y(s)$ are given, the position $(\mathbf{c}(s))$ and the posture $(\mathbf{e}_r(s), \mathbf{e}_p(s), \mathbf{e}_y(s))$ of the track are obtained as the solution of (1). Fig. 3(b) shows a visualized image of a solution.

Now we consider the starting point of the track as the head (or tail) of a snake-like robot, and consider $\mathbf{c}(s)$ and $(\mathbf{e}_r(s), \mathbf{e}_p(s), \mathbf{e}_y(s))$ as the position and the posture of its body respectively. Thus we can translate the track to the shape of the snake-like robot. We call the set of $\mathbf{c}(s)$ and $(\mathbf{e}_r(s), \mathbf{e}_p(s), \mathbf{e}_y(s))$ a "dorsal reference curve", because its shape (Fig. 3(b)) reminds us a slender fish that has a dorsal fin. In addition we call $\tau(s), \kappa_p(s), \kappa_y(s)$ shape functions.

We assume that a dorsal reference curve in this paper always satisfies $\tau(s) = 0$, because we consider a snake-like robot which doesn't twist.

III. KINEMATICS OF STEERING OF PEDAL WAVE

A. Steering by Superposition of Curvatures

First, we define a shape of pedal wave without steering. A dorsal reference curve of pedal wave forms vertical waves, therefore $\kappa_p(s)$ should be a cyclic function whose average is 0. Though any function is available if it satisfies the above condition, we use a sine function because it is smooth and has been used in our prior research. The shape functions for straight pedal wave are as follows;

$$\kappa_p(s) = \frac{2\pi}{L_p}\alpha_p \sin\frac{2\pi}{L_p}s \quad (2)$$

$$\kappa_y(s) = 0, \quad (3)$$

where α_p is a maximum angle between the body and the direction of movement and L_p is the wavelength. Fig. 1 shows an example of this shape. This curve is called a serpenoid.

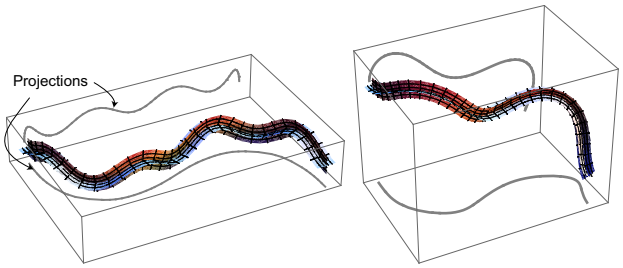

(a) A successful case ($L = 4L_p$) (b) A failed case ($L = 2L_p$)

Fig. 4. Shapes of pedal wave with horizontal steering curvature

Second, we see if it is possible to bend this shape around the vertical axis by adding some appropriate value to $\kappa_y(s)$. Now we test the following function.

$$\kappa_y(s) = \frac{2\pi}{L}\alpha \sin \frac{2\pi}{L}s \tag{4}$$

This is also a sine function and Fig. 4a shows the shape when $\alpha = \pi/3$ and $L = 4L_p$. The dorsal reference curve bent smoothly around the vertical axis while it kept the shape of pedal wave. Therefore, we propose the following shape functions for steering of pedal wave considering the change of the time;

$$\kappa_{pw}(s,t) \equiv \frac{2\pi}{L_p}\alpha_p \sin 2\pi\left(\frac{s}{L_p} - \frac{t}{T_p}\right) \tag{5}$$

$$\kappa_p(s,t) = \kappa_{sp}(s+vt) + \kappa_{pw}(s,t) \tag{6}$$

$$\kappa_y(s,t) = \kappa_{sy}(s+vt), \tag{7}$$

where t is the time, T_p is a period of pedal wave, v is a velocity of movement by pedal wave, $\kappa_{pw}(s,t)$ is the pedal wave's curvature, and $\kappa_{sp}(s,t)$ and $\kappa_{sy}(s,t)$ are the vertical and horizontal steering curvature respectively. We note that the shape functions are superposition of curvatures of pedal wave and steering. The reason why κ_{sp} and κ_{sy} are functions of $s + vt$ is that the steering curvatures should travel along the body synchronously with the movement by pedal wave.

However, the shape obtained by the above equations is not always appropriate. For example, when we choose $L = 2L_p$ at (4), the dorsal reference curve becomes different from both of pedal wave and the steering curve, and not suitable for pedal wave. In general, when we design a curve by superposition of curvatures of 2 different curves, the new curve does not necessarily have the same feature as original curves, because the curvatures and the shape of curve complexly affect each other as shown by (1). However, speaking from experience, the above method is available when we combine curvatures which have much different wavelength like the example shown in Fig. 4a. Therefore we investigate the condition of the appropriate steering curvature quantitatively in this section. We use numerical simulations here because analytical approach is difficult due to the complexity of (1).

B. Evaluation of Pedal Wave's Shape

First, we consider the following 2 conditions of appropriate pedal wave.

1) The dorsal reference curves forms vertical waves.
2) The average position and direction of the dorsal reference curve don't change significantly when the phase of pedal wave changes.

The condition (2) needs supplementary explanation. When a robot is moving with pedal wave, its phase (the value inside the parentheses of (5)) changes as time passes. Therefore, the shape of the dorsal reference curve around the area where the steering curvature is not zero can change significantly. The condition (2) means that this change should be small. For example, the shape shown in Fig. 4b is inappropriate because it doesn't satisfy the condition (1). However, it is difficult to test the condition (1) quantitatively, we use condition (2) in this paper. It is empirically sufficient because a shape satisfying (2) also satisfies (1) in our experience.

C. Calculation of Changes of Position and Direction

Now we describe how to evaluate changes of position and direction of a dorsal reference curve. We set the steering area between point O ($s = 0$) and point A ($s = s_i$), and assume that the steering curvatures are 0 outside this area (Fig. 5). The change of the position is calculated as the change of average position between point A and point B. Now we assume that the distance between A and B is L_p (wavelength of pedal wave) and B is outside the steering area. Therefore the average position of a curve between A and B is obtained as follows;

$$\mathbf{c}_{ave}(t) = \left(\frac{\int_{s_i}^{s_f} c_x(s,t)ds}{L_p}, \frac{\int_{s_i}^{s_f} c_y(s,t)ds}{L_p}, \frac{\int_{s_i}^{s_f} c_z(s,t)ds}{L_p}\right), \tag{8}$$

where $s_f = s_i + L_p$ and $\{c_x(s,t), c_y(s,t), c_z(s,t)\}$ indicates the position vector of the dorsal reference curve calculated by (1). Next we define $\bar{\mathbf{c}}_{ave}$ as the average of $\mathbf{c}_{ave}(t)$ and R_e as the maximum value of $||\mathbf{c}_{ave}(t) - \bar{\mathbf{c}}_{ave}||/L_p$ during one cycle. They are calculated as follows;

$$\bar{\mathbf{c}}_{ave} = \frac{1}{T_p}\int_0^{T_p} \mathbf{c}_{ave}(t)dt \tag{9}$$

$$R_e = \max_{t\in[0,T_p]}(||\mathbf{c}_{ave}(t) - \bar{\mathbf{c}}_{ave}||/L_p), \tag{10}$$

where $||\cdot||$ means the norm of a vector and (9) means that each component of $\mathbf{c}_{ave}(t)$ is integrated. The reason why we use L_p to normalize distance at (10) is that L_p is usually a constant value for each robot. This definition shows that the average position of the curve ($\mathbf{c}_{ave}(t)$) is always in the sphere with a radius of $R_e \cdot L_p$. Therefore when the shape of the curve is appropriate, R_e is small. However, even when R_e is small the shape is not always suitable, because the rolling of curve doesn't affect R_e. Hence we introduce $\Delta\theta$ which evaluates the change of the angle ($\theta(t)$) between the vertical axis of the absolute coordinate system and pitch axis at point B (Fig. 5). $\Delta\theta$ is defined as the difference between the maximum and minimum value of $\theta(t)$ during one cycle.

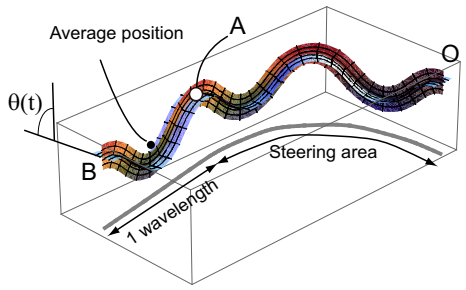

Fig. 5. Setting for evaluation

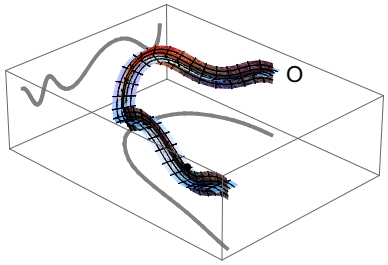

Fig. 6. A shape with horizontal steering curvature ($L_p/L = 0.25$, $\beta = \pi$, $\alpha_p = \pi/6$)

In addition, we have to adjust the position and direction of a dorsal reference curve at point O as follows in order to cancel the movement of pedal wave;

$$c_x(0,t) = c_y(0,t) = 0 \quad (11)$$

$$c_z(0,t) = c_z^s(-t/T_p \cdot L_p, 0) \quad (12)$$

$$\mathbf{e}_r(0,t) = \left\{\cos\left(\alpha_p \cos\frac{2\pi t}{T_p}\right), 0, \sin\left(\alpha_p \cos\frac{2\pi t}{T_p}\right)\right\} \quad (13)$$

$$\mathbf{e}_p(0,t) = (0,1,0), \quad (14)$$

where $c_z^s(s,t)$ is a z-coordinate of a dorsal reference curve when steering curvatures are 0.

The permissible range of R_e and $\Delta\theta$ can be change according to circumstances. However, in this paper we empirically decide the permissible range as $R_e < 0.1$ and $\Delta\theta < 0.2$ rad (11deg). Some examples of the evaluation are shown in the video attachment.

1) Horizontal Steering: We investigate R_e and $\Delta\theta$ when we superpose a horizontal steering curvature. The steering curvature is given by a half of serpenoid as follows;

$$\kappa_{sp}(s) = 0 \quad (15)$$

$$\kappa_{sy}(s) = \begin{cases} \frac{\pi}{L}\beta \sin\frac{2\pi}{L}s & (s < L/2) \\ 0 & (L/2 \le s) \end{cases}, \quad (16)$$

where β is the amplitude of steering. The reason why we chose sine is that it connects the straight area and the steering curve smoothly and that it is convenient to investigate the condition about wavelength. Fig. 6 shows the shape when $\alpha = \pi/6$, $\beta = \pi/2$ and $L_p/L = 0.25$, and Fig. 7 shows R_e and $\Delta\theta$ when $\alpha_p = \pi/3$. Fig. 7 shows that when $|\beta|$ and L_p/L are small, R_e and $\Delta\theta$ become small. In addition, we also confirmed that when α_p is small R_e and $\Delta\theta$ becomes small. Considering that we can't make $|\beta|$ small in order to steer, we obtained the condition of $L_p/L \le 0.25$ for an appropriate steering curvature according to the permissible range ($R_e < 0.1L_p$ and $\Delta\theta < 0.2$) which we decided above. We checked this condition holds true when $\alpha_p \le \pi/2$.

Moreover, we found that R_e and $\Delta\theta$ are often included within the permissible range even when we superpose curvatures of serpenoid which satisfy $L_p/L \le 0.25$. For example, Fig. 8 shows the shape of a dorsal reference curve with steering curvature made of superposition of 2 serpenoid ($\beta = \pi/2$ and $L_p/L = 0.25$ in the first curve, and $\beta = -2\pi/3$ and $L_p/L = 0.25$ in the second one, and the start position of the second one was $s = L/2$). The result was $R_e = 0.08$ and $\Delta\theta = 0.08$. This fact indicates that pedal wave can be freely steered to a certain extent by superposition of curvatures of serpenoid satisfying $L_p/L \le 0.25$.

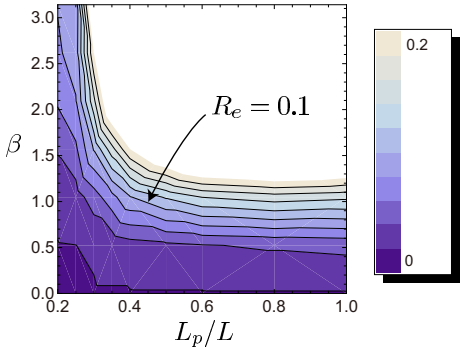

(a) R_e ($\alpha_p = \pi/3$)

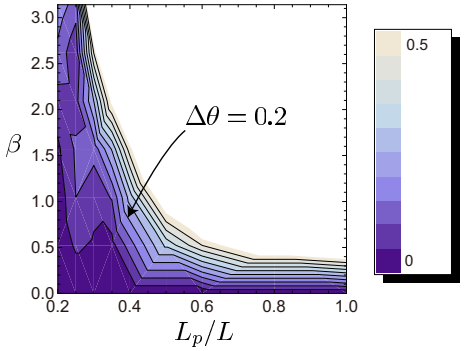

(b) $\Delta\theta$ ($\alpha_p = \pi/3$)

Fig. 7. R_e and $\Delta\theta$ in horizontal steering

2) Vertical Steering: We investigate R_e in vertical steering. In this case $\Delta\theta$ is always 0. First, as we did in horizontal steering we give the steering curvature by a half of serpenoid as follows.

$$\kappa_{sp}(s) = \begin{cases} \frac{\pi}{L}\beta \sin\frac{2\pi}{L}s & (s < L/2) \\ 0 & (L/2 \le s) \end{cases} \quad (17)$$

$$\kappa_{sy}(s) = 0 \quad (18)$$

Fig. 9 shows the result at $\alpha = \pi/6$ and $\pi/3$. These results shows that when α, $|\beta|$ and L_p/L are small, R_e becomes small in the same way as horizontal steering. However, R_e

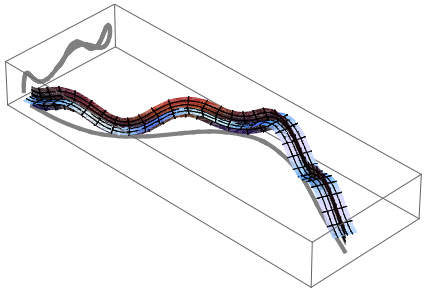

Fig. 8. A shape with superposition of horizontal steering curvature

TABLE I
SPECIFICATIONS OF ACM-L2

Size (L, W, H)	Weight	DOF	Max.torque	Max. angle
800, 46, 50 [mm]	1.0 kg	20	0.5 N·m	75deg

is wholly smaller than that of horizontal steering. Generally speaking, we can assume $|\beta| < \pi/2$ in (18) because the purpose of this steering is adaptation to uneven terrain. Considering this condition, the permissible range is decided as $L_p/L < -0.46\alpha + 1$ when $\alpha \leq \pi/3$.

Second, we investigate the following curvature whose purpose is obstacle climbing.

$$\kappa_{sp}(s) = \begin{cases} -\frac{\pi}{L}\beta \sin\frac{2\pi}{L}s & (s < L) \\ 0 & (L \leq s) \end{cases} \quad (19)$$

$$\kappa_{sy}(s) = 0 \quad (20)$$

Fig. 10a shows R_e at $\beta = \pi/2$. L_p/L should be large to fit the shape into an obstacle precisely, while α_p should not be too small to keep the velocity of pedal wave. Though the selection of L_p/L and α_p depends on circumstances, we consider $L_p = 0.7$ and $\alpha_p = 0.4$ is one of well-balanced options. Fig. 10b shows a shape at $\beta = \pi/2$, $L_p/L = 0.7$ and $\alpha_p = 0.4$.

IV. EXPERIMENTS

We conducted experiments to verify the proposed steering method. Table I shows the specification of "ACM-L2", which we used in the experiments. ACM-L2 is composed of "double joints" proposed in our prior research[12]. A snake-like robot composed of double joints can form a similar shape of a dorsal reference curve[13]. Fig. 11 shows the approximation of the shape shown in Fig. 8. The joint angles are calculated in a PC and the target angles are sent to micro computers in joint units (Fig. 12). The micro computers conduct position feedback control to realize the target angles.

Before experiments we measured the velocity of movement by pedal wave, which depended on α_p, L_p and friction of the environment. As the result we confirmed that the robot moved $0.2L_p$ during one cycle at $\alpha_p = 0.44$ rad (25deg), therefore we substituted $v = 0.2L_p/T_p$ in (6) and (7). In addition, the parameters were chosen as $\alpha_p = 0.44$ and $L_p = 273$ mm in the experiments.

First we tested horizontal steering by (16). The wavelength of steering curvature was fixed at $L_p/L = 0.25$ and its amplitude and timing was input by the operator using joysticks. As shown in Fig. 13a the robot successfully went through obstacles by horizontal steering. However, we note that because the wavelength of steering curvature was not small ($L = 1.1$ m), the operation of steering was relatively difficult.

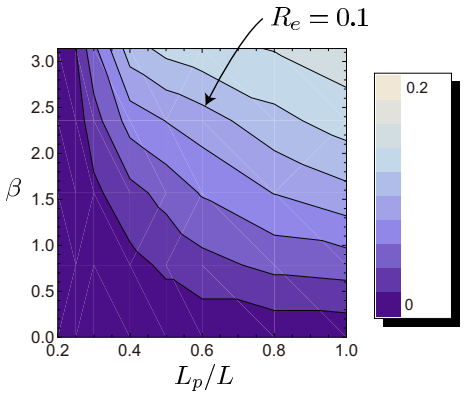

(a) R_e ($\alpha_p = \pi/6$)

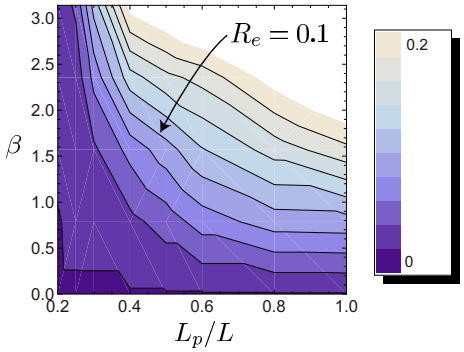

(b) R_e ($\alpha_p = \pi/3$)

Fig. 9. R_e in vertical steering

Second, we conducted vertical steering for climbing over an obstacle. The wavelength of steering curvature was fixed by $L_p/L = 0.67$ and its amplitude and timing was inputted by an operator using joysticks in the same way as the first experiment. As the result the robot successfully went over an obstacle of 60mm in height as shown in Fig. 13b. However, this shape was easy to fall down and it was difficult to go over obstacles which are higher than 60mm. The scenes of above experiments are included in the video attachment.

V. CONCLUSION

This paper described steering method of pedal wave of a snake-like robot. First, we showed that steering can be realized by superposition of steering curvatures and pedal-wave's curvature. Second, the limitation of steering curvature was investigated quantitatively. As the result, it was clarified that the wavelength of steering curvature has to be large compared to that of pedal-wave's wavelength. Furthermore we verified the proposed idea by experiments. We believe that the proposed steering method is so simple that it can be applied to various types of snake-like robots.

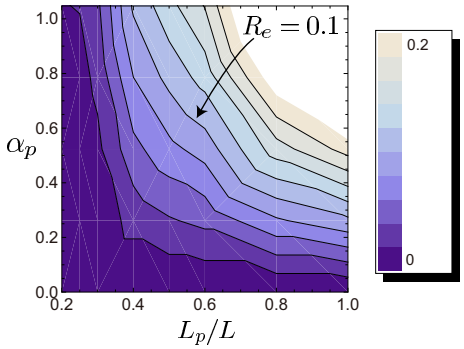

(a) R_e ($\beta = \pi/2$)

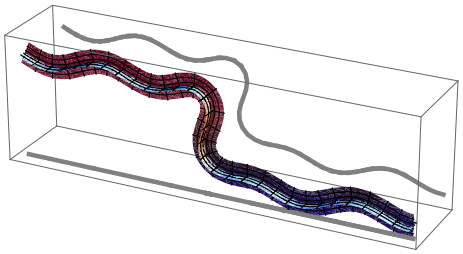

(b) Shape ($L_p/L = 0.7, \beta = \pi/2, \alpha_p = 0.4$)

Fig. 10. Pedal wave with vertical steering for obstacle climbing

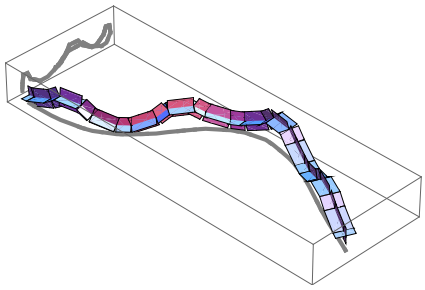

Fig. 11. Approximation by a structure composed of double joints (12 joints)

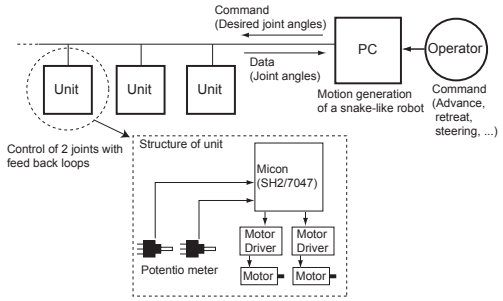

Fig. 12. Control system of ACM-L2

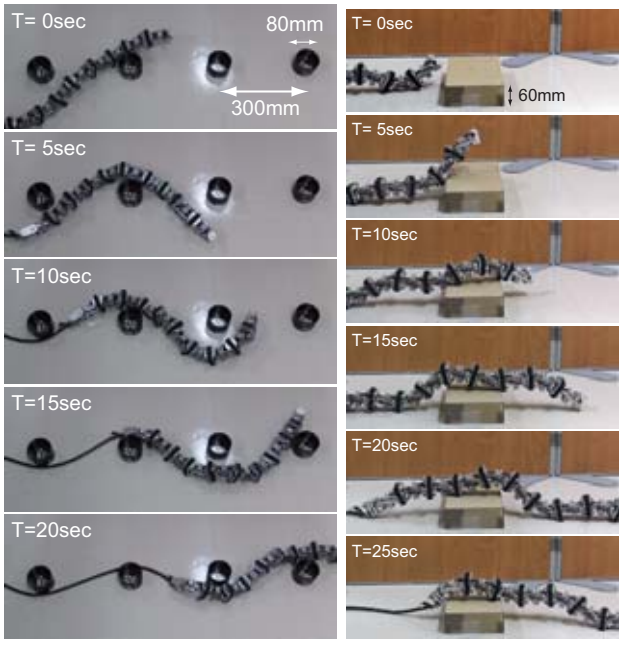

(a) horizontal steering (b) obstacle climbing

Fig. 13. Experiments of steering

In future work we will study the mechanism and control of a snake-like robot which utilize pedal wave and has a high mobility in narrow and complicated environments.

VI. ACKNOWLEDGMENTS

This research was partially supported by Ministry of Education, Science, Sports and Culture, Grant-in-Aid for Scientific Research(A), No. 18206026.

REFERENCES

[1] S. Hirose, "Biologically Inspired Robots", *Oxford University Press*, 1993.

[2] G. S. Chirikjian, Joel W. Burdick, "The Kinematics of Hyper-Redundant Robot Locomotion", *IEEE Transaction on Robotics and Automation*, vol. 11, No. 6, pp.781-793, 1995.

[3] H. W. Lissmann, "Rectilinear Locomotion in a Snake (Boa Occidentalis)", J. of Experimental Biology, Vol.26, pp.368-379, 1950.

[4] M. Yim, K. Roufas, S. Homans, "Climbing with snake-like robots", *Proc. of the IFAC Workshop on Mobile Robot Technology*, 2001.

[5] H. Ohno, S. Hirose, " Design of Slim Slime Robot and its Gait of Locomotion", *Proc. of the 2001 IEEE Int. Conf. on Intelligent Robots and Systems*, pp.707-715, 2001.

[6] A. Kamimura, H. Kurokawa, E. Yoshida, S. Murata, K. Tomita, S. Kokaji, " Automatic Locomotion Design and Experiments for a Modular Robotic System ", *IEEE Transaction on Mechatronics*, Vol.10, No.3, pp.314-325, 2005.

[7] G. S. Chirikjian, J. W. Burdick, "A Modal Approach to Hyper-Redundant Manipulator Kinematics", *IEEE Transaction on Robotics and Automation*, vol. 10, No. 3, pp343-354, 1994.

[8] H.Yamada, S.Hirose, "Study of Active Cord Mechanism (Approximations to continuous curves of a multi-joint body)", *J. of the Robotics Society of Japan*, Vol.26, No.1, pp.110-120, 2008. (In Japanese)

[9] M. Mori, H. Yamada, S. Hirose, "Design and Development of Active Cord Mechanism "ACM-R3" and its 3-dimensional Locomotion Control", *J. of the Robotics Society of Japan*, Vol.23, No.7, pp.886-897, 2005. (In Japanese)

[10] H. Yamada, S. Hirose, "Study on the 3D Shape of Active Cord Mechanism", *Proc. of 2006 IEEE Int. Conf. on Robotics and Automations*, pp.2890-2895, 2006.

[11] A. E. H. Love, "A Treatise on the mathematical theory of elasticity," *Cambridge University Press*, 1927.

[12] H. Yamada, S. Hirose: "Study of a 2-DOF Joint for the Small Active Cord Mechanism", *Proc. of 2009 IEEE Int. Conf. on Robotics and Automations*, pp.3827-3832, 2009.

[13] H. Yamada, S. Hirose: "Approximations to Continuous Curves of Active Cord Mechanism Made of Arc-shaped joints or Double Joints", *Proc. of 2010 IEEE Int. Conf. on Robotics and Automations*, pp.703-708, 2010.